R. J., Batlogg, B., Rupp., L. W., Ansaldo, E. J., and William, D. L., 1989, "Magnetic Penetration Depth in Single-Crystal $YBa_2Cu_3O_{7-\delta}$," *Phys. Rev. B*, Vol. 39, pp. 851–854.

Kamaras, K., Herr, S. L., Porter, C. D., Tanner, D. B., Etemad, S., and Chan, S. W., 1989, "Optical Excitations in Thin Film $YBa_2Cu_3O_7$," in: *Progress in High Temperature Superconductivity*, Vol. 17, L. H. Bennet, Y. Flom, and G. C. Vezzoli, eds., World Scientific Publishing Co., Singapore.

Kamaras, K., Herr, S. L., Porter, C. D., Tache, N., Tanner, D.B., Etemad, S., Venkatesan, T., Chase, E., Inam, A., Wu, X. D., Hegde, M. S., and Dutta, B., 1990, "In a Clean High-T_c Superconductor You Do Not See the Gap," *Phys. Rev. Lett.*, Vol. 64, pp. 84–87.

Leplae, L., 1983, "Derivation of an Expression for the Conductivity of Superconductors in Terms of the Normal-State Conductivity," *Phys. Rev. B*, Vol. 27, pp. 1911–1912.

Lee, A. E., Platt, C. E., Burch, J. F., and Simon, R. W., 1990, "Epitaxially Grown Sputtered $LaAlO_3$ Films," *Appl. Phys. Lett.*, Vol. 57, pp. 2019–2021.

Lee, W., Rainer, D., and Zimmermann, W., 1988, "Quasiclassical Linear Response Theory," *Internal Report*, Theoretical Physics III, Physikalisches Institut, University of Bayreuth, D-8580 Bayreuth, Germany.

Lee, W., Rainer, D., and Zimmermann, W., 1989, "Holstein Effect in the Far-Infrared Conductivity of High-T_c Superconductors," *Physica C*, Vol. 159, pp. 535–544.

Mattis, D. C., and Bardeen, J., 1958, "Theory of the Anomalous Skin Effect in Normal and Superconducting Metals," *Phys. Rev.*, Vol. 111, pp. 412–417.

Mikic, B. B., 1974, "Thermal Contact Conductance; Theoretical Considerations," *Int. J. Heat Mass Transfer*, Vol. 17, pp. 205–214.

Mogro-Campero, A., and Tumer, L. G., 1991, "Lower Temperature Postannealing of Thin Films of $YBa_2Cu_3O_7$ at Lower Oxygen Partial Pressure," *Appl. Phys. Lett.*, Vol. 58, pp. 417–418.

Olsen, J. L., 1962, *Electron Transport in Metals*, Interscience Publishers, New York, Chap. 4.

Orenstein, J., Thomas, G. A., Millis, A. J., Cooper, S. L., Rapkine, D. H., Timusk, T., Schneemeyer, L. F., and Waszczak, J. V., 1990, "Frequency- and Temperature-Dependent Conductivity in $YBa_2Cu_3O_{6+x}$ Crystals," *Phys. Rev. B*, Vol. 42, pp. 6342–6362.

Phelan, P. E., Flik, M. I., and Tien, C. L., 1991, "Radiative Properties of Superconducting Y–Ba–Cu–O Thin Films," ASME JOURNAL OF HEAT TRANSFER, Vol. 113, pp. 487–493.

Phelan, P. E., Chen, G., and Tien, C. L., 1992, "Thickness-Dependent Radiative Properties of Y–Ba–Cu–O Thin Films," ASME JOURNAL OF HEAT TRANSFER, Vol. 114, pp. 227–233.

Rao, A. M., Eklund, P. C., Lehman, G. W., Face, D. W., Doll, G. L., Dresselhaus, G., and Dresselhaus, M. S., 1990, "Far-Infrared Optical Properties of Superconducting $Bi_2Sr_2CaCu_2O_x$ Films," *Phys. Rev. B*, Vol. 42, pp. 193–201.

Renk, K. R., Eschrig, H., Hofmann, U., Keller, J. Schützmann, J., and Ose, W., 1990, "Dynamical Conductivity of High-T_c Superconductors," *Physica C*, Vol. 165, pp. 1–7.

Schlesinger, Z., Collins, R. T., Holtzberg, F., Feild, C., Koren, G., and Gupta, A., 1990, "Infrared Studies of the Superconducting Energy Gap and Normal-State Dynamics of the High-T_c Superconducting $YBa_2Cu_3O_7$," *Phys. Rev. B*, Vol. 41, pp. 11237–11259.

Schützmann, J., Ose, W., Keller, J., Renk, K. F., Roas, B., Schultz, L., and Saemann-Ischenko, G., 1989, "Far-Infrared Reflectivity and Dynamical Conductivity of an Epitaxial $YBa_2Cu_3O_{7-\delta}$ Thin Film," *Europhys. Lett.*, Vol. 8, pp. 679–684.

Sengupta, L. C., Huang, D., Roughani, B., Aubel, J. L., and Sundaram, S., 1991, "Spectroscopic Ellipsometry Studies of $YBa_2Cu_3O_{7-\delta}$ Deposited on $SrTiO_3$," *J. Appl. Phys.*, Vol. 69, pp. 8272–8276.

Siegal, M. P., Phillips, J. M., van Dover, R. B., Tiefel, T. H., and Marshall, J. H., 1990a, "Optimization of Annealing Parameters for Growth of Epitaxial $Ba_2YCu_3O_{7-x}$ Films on $LaAlO_3$ (100)," *J. Appl. Phys.*, Vol. 68, pp. 6353–6360.

Siegal, M. P., Phillips, J. M., Hsieh, Y.-F., and Marshall, K. "Growth of Epitaxial $Ba_2YCu_3O_{7-x}$ Films on $LaAlO_3$ (100)," Vol. 172, pp. 282–286.

Siegel, R., and Howell, J. R., 1981, *Thermal Radiation Heat Tr* ed., McGraw-Hill, New York, Chap. 19.

Terashima, T., Shimura, K., Bando, Y., Matsuda, Y., Fujiyam Komiyama, S., 1991, "Superconductivity of One-Unit-Cell Thick Thin Film," *Phys. Rev. Lett.*, Vol. 67, pp. 1362–1365.

Timusk, T., Herr, S. L., Kamaras, K., Porter, C. D., Tanner, D. B., Bonn, D. A., Garrett, J. D., Stager, C. V., Greedan, J. E., and Reedyk, M., 1988, "Infrared Study of *ab*-Plane Oriented Oxide Superconductors," *Phys. Rev. B*, Vol. 38, pp. 6683–6688.

Timusk, T., and Tanner, D. B., 1989, "Infrared Properties of High-T_c Superconductors," in: *Physical Properties of High-Temperature Superconductors I*, D. M. Ginsberg, ed., World Scientific Publishing Co., Singapore, pp. 339–407.

Tinkham, M., 1970, "Far Infrared Absorption in Superconductors," in: *Far-Infrared Properties of Solids*, S. S. Mitra and S. Nudelman, eds., Plenum Press, New York, pp. 223–246.

Toscano, W. M., and Cravalho, E. G., 1976, "Thermal Radiation Properties of the Noble Metals at Cryogenic Temperatures," ASME JOURNAL OF HEAT TRANSFER, Vol. 98, pp. 438–445.

Van der Marel, D., Habermeier, H.-U., Heitmann, D., König, W., and Wittlin, A., 1991, "Infrared Study of the Superconducting Phase Transition in $YBa_2Cu_3O_{7-x}$," *Physica C*, Vol. 176, pp. 1–18.

Wooten, F., 1972, *Optical Properties of Solids*, Academic Press, New York, Chap. 6.

Xi, X. X., Geerk, J., Linker G., Li, Q., and Meyer, O., 1990, "Preparation and Superconducting Properties of Ultrathin $YBa_2Cu_3O_{7-x}$ Films," *Appl. Phys. Lett.*, Vol. 54, pp. 2367–2369.

Zhang, K., Bunker, G. B., Zhang, G., Zhao, Z. X., Chen, L. Q., and Huang, Y. Z., 1988, "Extended X-Ray Absorption Fine-Structure Experiment on the High-T_c Superconductor $YBa_2Cu_3O_{7-\delta}$," *Phys. Rev. B*, Vol. 37, pp. 3375–3380.

Ziman, J. M., 1960, *Electrons and Phonons*, Oxford University Press, Oxford, United Kingdom, Chap. 9.

Zimmermann, W., Brandt, E. H., Bauer, M., Seider, E., and Genzel, L., 1991, "Optical Conductivity of BCS Superconductors With Arbitrary Purity," *Physica C*, Vol. 183, pp. 99–104.

Evaluation of Total Emittance of an Isothermal Nongray Absorbing, Scattering Gas–Particle Mixture Based on the Concept of Absorption Mean Beam Length

W. W. Yuen

A. Ma

Department of Mechanical and Environmental Engineering, University of California, Santa Barbara, CA 93106

A general methodology to evaluate the total emittance of an isothermal, nongray, isotropically scattering particle–gas mixture is illustrated. Based on the concept of absorption mean beam length (AMBL), the methodology is demonstrated to be computationally efficient and accurate. As an illustration, the total emittance of a slab containing carbon particles and CO_2 is evaluated. The nongray extinction coefficient and scattering albedo of carbon particles are calculated based on Mie theory and the available index of refraction data. The narrow-band fixed-line-spacing model (Edwards et al., 1967) is used to characterize the nongray spectral absorption coefficient of CO_2. Numerical data show that the combined nongray and scattering effects are quite significant. For particles with moderate and large radius (say, ≥ 1 μm), ignoring the effect of scattering can lead to error in the prediction of total emittance by more than 20 percent. The no-scattering results also yield incorrect qualitative behavior of the total emittance in terms of its dependence on the mixture temperature and particle concentration. The accuracy of many of the existing predictions of total emittance of gas-particle mixtures that ignore the scattering effect is thus highly uncertain.

1 Introduction

In the assessment of performance of high-temperature engineering equipment such as industrial furnaces, the ability to predict accurately the radiative emission from a mixture of particles and gas is essential. Until now, this essential ability has been limited largely to absorbing particles and gas mixtures. With available spectroscopic absorption data for various gases and particles, together with the concept of mean beam length (MBL) originally introduced by Hottel (1927), accurate predictions of total emittance of multidimensional nongray absorbing gas–particle mixtures are now accepted as routine. Two important factors contribute to the success of these efforts. First, reasonably reliable spectral absorption data are now available for most gases. Second, MBL has been shown to be primarily a function only of geometry (i.e., independent of wavelength) and can be, to a good approximation, considered as constant in a nongray calculation. The necessary spectral integration is thus reduced to a one-dimensional form and can be readily evaluated.

The success in estimating the radiative emission from a nongray absorbing, scattering particle–gas mixture, on the other hand, has been quite limited. The primary difficulty is that even when the medium can be considered as gray, accurate numerical solution to the radiative transfer equation is difficult to obtain. Many approximation methods (see the review article by Viskanta and Menguc, 1987) have been proposed. The accuracy of such methods, however, is generally unknown. For nongray analysis, two general approaches are utilized. In one approach (Menguc and Viskanta, 1986), the computational method developed for a gray analysis is extended to the nongray case by the Hottel's MBL concept. This extension, however, is done on an ad hoc basis. Without a rigorous theoretical justification, the accuracy of this approach is highly uncertain. The second approach is to develop approximate solution techniques directly for the nongray analysis (Skocypec and Buckius, 1984). While this approach has been successful in generating numerical data for a few selected problems (say, parallel slab geometry), the applicability of the method to analysis of general enclosures is uncertain. The accuracy of all existing solution approaches is also difficult to assess because of the lack of reliable "benchmark" numerical data for direct comparison.

The objective of this work is to show that utilizing the concept of absorption mean beam length (AMBL) (Yuen, 1990, 1991), a general methodology can be developed for the evaluation of radiative emission from a nongray absorbing-scattering particle–gas mixture. The methodology is computationally efficient, accurate, and applicable to enclosures with arbitrary geometry. As an illustration, the total emittance of a carbon particles/CO_2 containing slab is calculated. In addition to generating a set of numerical data, which serves as a benchmark set of "exact" results for this class of problem, the importance of the scattering effect on the total emittance is also illustrated quantitatively.

2 Analysis

A schematic of the general methodology for the evaluation of total emittance of a nongray absorbing-scattering particle–gas mixture is shown in Fig. 1. Similar to the MBL approach, which was successful for the evaluation of total emittance of a nonscattering medium, the fundamental principle of the methodology is to separate the geometric effect and the spectral effect in the numerical integration. Except for the increased complexity in the evaluation of AMBL, the present approach

Contributed by the Heat Transfer Division for publication in the JOURNAL OF HEAT TRANSFER. Manuscript received by the Heat Transfer Division April 1991; revision received February 1992. Keywords: High-Temperature Phenomena, Modeling and Scaling, Radiation. Associate Technical Editor: R. O. Buckius.

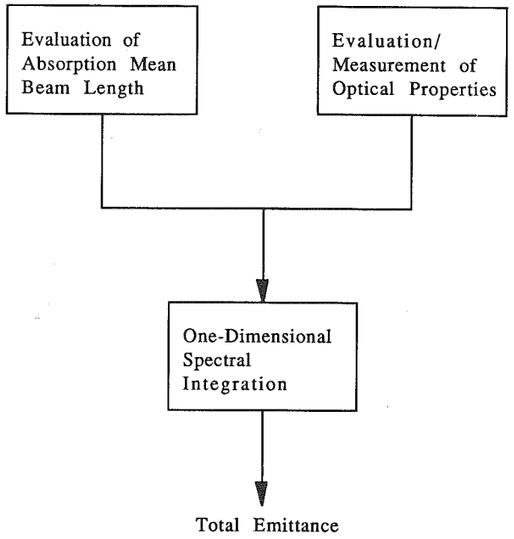

Fig. 1 Schematics of the general methodology for the evaluation of total emittance of an absorbing/scattering particle-gas mixture

has the same degree of mathematical complexity as the conventional MBL approach.

2.1 Evaluation of AMBL. As shown in earlier work (Yuen, 1990, 1991), AMBL is the radius of an equivalent purely absorbing and emitting hemisphere such that the heat flux evaluated at the center of its base is identical to the actual heat flux. For an isothermal medium with a known geometry, temperature T, and optical properties (i.e., absorption coefficient a_λ, scattering albedo ω_λ and scattering phase function); the spectral heat transfer, q_λ, can be calculated by standard numerical techniques developed for a gray medium, e.g., the Monte Carlo Method (Howell and Perlmutter, 1964), the Zonal/Network Method (Hottel and Sarofim, 1967; Yuen, 1990) for isotropically scattering media and Generalized Zonal Method (Yuen and Takara, 1990) for anisotropically scattering media. The mathematical definition of AMBL, $L_{ab,\lambda}$, is given by

$$q_\lambda = e_{\lambda,b}(T)(1 - e^{-a_\lambda L_{ab,\lambda}}) \tag{1}$$

For an isothermal slab and with the assumption that the scattering is isotropic, AMBL calculated for the radiative heat transfer to one of its surfaces (Yuen, 1991) is presented in Fig. 2. Note that the mathematical behavior of AMBL is quite different from that of Hottel's MBL. In contrast to MBL, for example, AMBL varies strongly with absorption coefficient

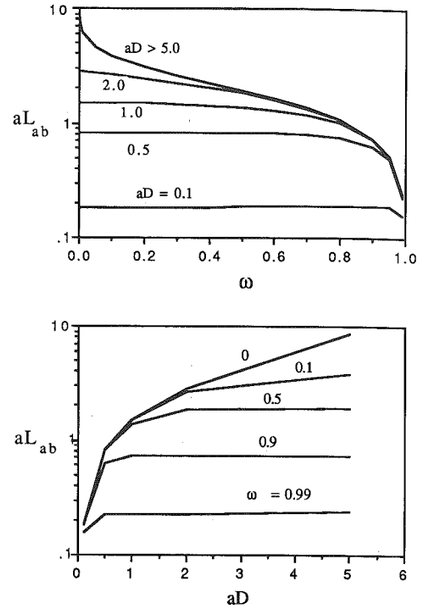

Fig. 2 Absorption mean beam length for a parallel slab with different absorption optical thickness, *aD*, and scattering albedo, ω

and scattering albedo. While MBL increases as the characteristic dimension of the physical system increases, AMBL approaches an asymptotic finite value in the optically thick limit for a medium with nonzero scattering albedo. Physically, MBL correlates approximately the optical "size" of the medium. AMBL, on the other hand, correlates only the optical "size" that contributes to the heat transfer. For a medium with a finite scattering albedo, increase in the physical dimension of the system will have less and less effect on AMBL since the additional medium has less and less influence on the overall heat transfer due to the effect of scattering. This explains the asymptotic behavior of AMBL in the optically thick limit. In the limit of a large scattering albedo. AMBL can be quite small even for a physically "large" system because the optical "size" that contributes to the heat transfer is small.

Fundamentally, the important function of AMBL is to account for the effect of enclosure geometry on radiation heat transfer without a simultaneous consideration of the detailed spectral properties of a specific mixture. The numerical data in Fig. 2, for example, account for the effect of the parallel slab geometry on radiation heat transfer over the entire range of radiation parameter. The same data can be used to analyze

Nomenclature

a_λ = absorption coefficient
B = gas absorption correlation parameters, Eq. (2)
C = gas absorption correlation parameters, Eqs. (2) and (3)
C_1 = gas absorption correlation parameters, Eqs. (3) and (4)
C_2 = gas absorption correlation parameters, Eq. (4)
C_3 = gas absorption correlation parameters, Eqs. (3) and (4)
d = gas absorption correlation parameters, Eqs. (2) and (5)
d_0 = gas absorption correlation parameters, Eq. (5)
$e_{\lambda,b}$ = blackbody emissive power
$L_{ab,\lambda}$ = absorption mean beam length
n = gas absorption correlation parameters, Eq. (6)
N = particle number density
P_A = partial pressure of the absorbing gas
P_B = partial pressure of the N_2 broadening gas
P_e = effective pressure parameter, Eq. (6)
P_0 = reference pressure = 1 atm
q_λ = heat flux
Q_{abs} = absorption cross section
Q_{sca} = scattering cross section
r = particle radius
T = temperature
T_0 = reference temperature = 100 K
ϵ_λ = emittance
κ = extinction coefficient
λ = wavelength
ρ = gas density, Eq. (2)
τ = transmissivity
ω = scattering albedo

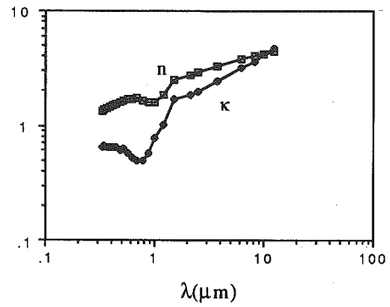

Fig. 3 Measured data on complex index of refraction ($n - ik$) for carbon

any isothermal mixture with the same geometry. Since AMBL is readily computable with established computational methods (developed for gray analysis) and the spectral integration is one dimensional, the overall computation is straightforward and requires little effort.

2.2 Evaluation of Spectral Optical Properties. This process can be readily accomplished utilizing well-established numerical procedures and/or experimental data. For many common absorbing gaseous species, for example, the narrow-band fixed-line-spacing model (Edwards et al., 1967) is known to be an effective engineering approximation for the nongray spectral absorption behavior. The gaseous absorption coefficient (suppressing the subscript λ for simplicity) is given by

$$a = \frac{\rho C^2 \sinh(\pi B^2 P_e/2)}{\cosh(\pi B^2 P_e/2) - \cos(2\pi\nu^*/d)} \tag{2}$$

where ν^* is the wavenumber measured from the center of the band, $C^2(\nu, T)$, $B^2(\nu, T)$, d and P_e are specified in terms of isothermal gas correlation parameters as

$$C^2 = (C_1/C_3)e^{-\nu^*/C_3} \tag{3}$$

$$B^2 = C_2^2/(4C_1C_3) \tag{4}$$

$$d = d_0 C_3(T_0), \quad T_0 = 100 \text{ K} \tag{5}$$

$$P_e = [(P_B + bP_A)/P_0]^n, \quad P_0 = 1 \text{ atm} \tag{6}$$

with P_A being the partial pressure of the absorbing gas and P_B the partial pressure of the N_2 broadening gas. The gas correlation parameters, C_1, C_2, C_3, b, and n are defined for various common gaseous species (e.g., CO_2, H_2O, CO, and CH_4) in standard reference (Edwards et al., 1967).

In the present work, the absorbing gas is assumed to be a CO_2/N_2 mixture at atmospheric pressure. Over the expected mixture temperature range (500 to 3000 K), numerical experiments show that the present calculation can predict the pure CO_2 emittance data from Hottel's chart (Hottel, 1967) to within 10 percent by setting $d_0 = 30$. This assumption is therefore used in the generation of all numerical data.

If carbon particles in the mixture are assumed to be spherical, the evaluation of optical properties is also straightforward utilizing Mie theory (Van der Hulst, 1957). Specifically, for the set of index of refraction ($n - ik$) data for graphite carbon (Phillips, 1977) as shown in Fig. 3, the absorption efficiency Q_{abs}, the extinction efficiency Q_{ext}, and scattering albedo $\omega = 1 - Q_{abs}/Q_{ext}$ can be readily calculated for different particle sizes utilizing computer programs provided in standard references (Bohren and Huffman, 1983). The absorption coefficient, a, and extinction coefficient, κ, can be generated from these efficiency factors by

$$a = N\pi r^2 Q_{abs} \qquad \kappa = N\pi r^2 Q_{ext} \tag{7}$$

and N being the particle's number density and r the particle radius. Numerical results are presented in Figs. 4(*a*), 4(*b*), and

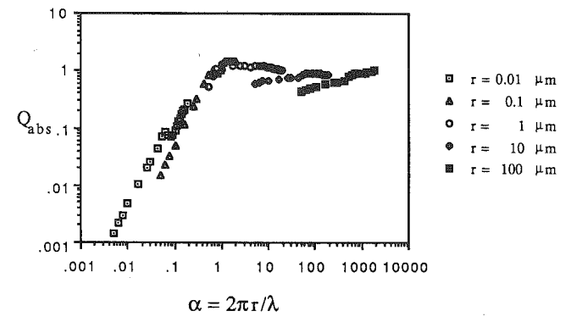

Fig. 4(*a*) Absorption efficiency for carbon particles of different radius

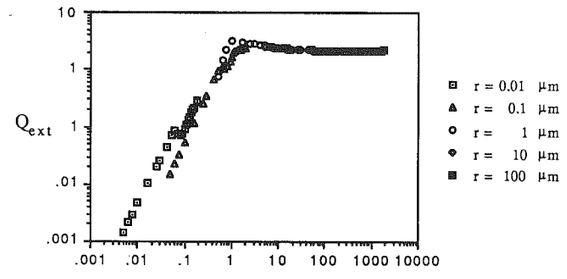

Fig. 4(*b*) Extinction efficiency for carbon particles of different radius

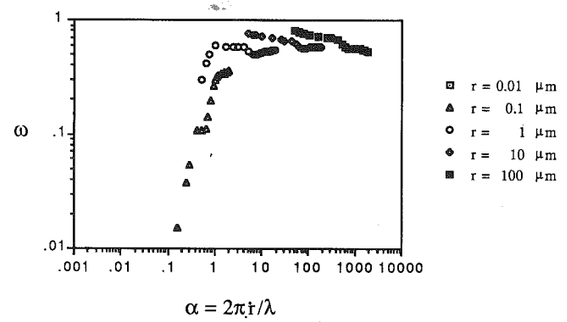

Fig. 4(*c*) Scattering albedo for carbon particles of different radius

4(*c*). It can be readily observed that the effect of scattering is quite significant when the particle radius is greater than 1 μm.

It is important to note that all results presented in this section are based on established information that is available from standard references. While the mixture characteristics are somewhat idealistic (pure CO_2 and spherical carbon particles) and differ from those of an actual combustion product mixture, the assumed mixture is sufficient to illustrate the effectiveness of the proposed methodology and the qualitative effect of scattering on the mixture's emittance. The adaptation of the present approach to a combustion medium with "real" properties is straightforward.

2.3 Integration to Obtain Total Emittance. Based on results generated from sections 2.1 and 2.2, the total emittance of a homogeneous gas–particle mixture can be written as

$$\epsilon = \frac{1}{\sigma T^4}\int_0^\infty e_{\lambda b}(T)(1 - e^{-a_{t,\lambda}L_{ab,\lambda}(a_{t,\lambda},\omega_{t,\lambda})})d\lambda \tag{8}$$

Table 1 Effect of temperature and number density on particle emittance, ϵ_p (values in parenthesis are generated ignoring the effect of scattering)

particle radius = 0.1 μm						
	T = 500 K	1000 K	1500 K	2000 K	2500 K	3000 K
ND = 10^{12}	0.00201 (0.00201)	0.00550 (0.00548)	0.0109 (0.0109)	0.0164 (0.0163)	0.0218 (0.0216)	0.0263 (0.0260)
10^{13}	0.0201 (0.0201)	0.0539 (0.0537)	0.102 (0.101)	0.146 (0.145)	0.182 (0.181)	0.213 (0.212)
10^{14}	0.177 (0.176)	0.334 (0.335)	0.504 (0.511)	0.618 (0.639)	0.686 (0.726)	0.724 (0.786)
particle radius = 1.0 μm						
	T = 500 K	1000 K	1500 K	2000 K	2500 K	3000 K
ND = 10^{10}	0.0342 (0.0335)	0.0354 (0.0347)	0.0343 (0.0335)	0.0337 (0.0329)	0.0336 (0.0328)	0.0338 (0.0330)
10^{11}	0.257 (0.258)	0.263 (0.266)	0.258 (0.262)	0.257 (0.260)	0.257 (0.260)	0.259 (0.262)
10^{12}	0.707 (0.838)	0.673 (0.874)	0.663 (0.887)	0.672 (0.903)	0.680 (0.913)	0.687 (0.920)
particle radius = 10 μ m						
	T = 500 K	1000 K	1500 K	2000 K	2500 K	3000 K
ND = 10^{8}	0.0325 (0.0318)	0.0341 (0.0335)	0.0362 (0.0355)	0.0386 (0.0378)	0.0406 (0.0398)	0.0422 (0.0413)
10^{9}	0.248 (0.251)	0.258 (0.261)	0.271 (0.273)	0.287 (0.289)	0.300 (0.301)	0.310 (0.310)
10^{10}	0.6583 (0.8773)	0.6759 (0.8787)	0.6999 (0.8921)	0.7295 (0.9144)	0.7511 (0.9281)	0.7666 (0.9362)

with $a_{t,\lambda}$ and $\omega_{t,\lambda}$ being the absorption coefficient and scattering albedo of the mixture given by

$$a_{t,\lambda} = a_{p,\lambda} + a_{g,\lambda} \tag{9}$$

and

$$\omega_{t,\lambda} = 1 - \frac{a_{t,\lambda}}{\kappa_{p,\lambda} + a_{g,\lambda}} \tag{10}$$

Note that the spectral AMBL, $L_{ab,\lambda}$, is evaluated based on the total absorption coefficient and total scattering albedo for the mixture. The subscript λ is inserted to emphasize the spectral dependence of all optical properties and the AMBL. For mathematical convenience, the total emittance can be separated into a particle emittance, ϵ_p, and a particle attenuated gas emittance, $\tau_p\epsilon_g$, by

$$\epsilon = \epsilon_p + \tau_p\epsilon_g \tag{11}$$

with

$$\epsilon_p = \frac{1}{\sigma T^4}\int_0^\infty e_{\lambda b}(T)(1 - e^{-a_{p,\lambda}L_{ab,\lambda}(a_{t,\lambda}\omega_{t,\lambda})})d\lambda \tag{12}$$

and

$$\tau_p\epsilon_g = \frac{1}{\sigma T^4}\int_0^\infty e_{\lambda b}(T)e^{-a_{p,\lambda}L_{ab,\lambda}(a_{t,\lambda}\omega_{t,\lambda})} (1 - e^{-a_{g,\lambda}L_{ab,\lambda}(a_{t,\lambda}\omega_{t,\lambda})})d\lambda \tag{13}$$

As in the utilization of conventional mean beam length for nonscattering media, AMBL reduces the spectral integration to an equivalent one-dimensional integral.

3 Results and Discussion

All numerical computations as outlined in sections 2.1, 2.2, and 2.3 are straightforward and can be carried out accurately and efficiently with little effort. Indeed, all numerical results presented in this work are generated either by a personal computer or a workstation and they are accurate to within a relative error of less than 1 percent. The present approach is thus particularly convenient for practical industrial applications.

Table 2 Particle emittance (in the optically thick limit), $\epsilon_{p,\infty,\lambda}$, for a particle–$N_2$ mixture and a particle–CO_2 mixture at different temperatures and particle sizes

particle radius = 0.1 μm				
	particle-CO_2 mixture			particle-N_2 mixture
λ (μm)	T = 1000K	2000K	3000K	
2.7	0.466	0.682	0.775	0.971
4.3	0.104	0.130	0.166	0.991
9.4	0.591	0.683	0.780	0.997
10.4	0.516	0.640	0.752	0.997
15.0	0.00360	0.0141	0.0311	0.997
particle radius = 1 μm				
	particle-CO_2 mixture			particle-N_2 mixture
λ (μm)	T = 1000K	2000K	3000K	
2.7	0.158	0.264	0.330	0.708
4.3	0.0781	0.0953	0.116	0.730
9.4	0.539	0.611	0.664	0.842
10.4	0.525	0.606	0.674	0.877
15.0	0.00489	0.0190	0.0410	0.942
particle radius = 10 μm				
	particle-CO_2 mixture			particle-N_2 mixture
λ (μm)	T = 1000K	2000K	3000K	
2.7	0.181	0.300	0.372	0.760
4.3	0.0748	0.0904	0.111	0.747
9.4	0.423	0.468	0.517	0.708
10.4	0.377	0.437	0.492	0.700
15.0	0.00665	0.0233	0.0458	0.691

3.1 Particle Emittance. The effect of temperature, particle radius, and particle number density on the particle emittance, ϵ_p, is illustrated by numerical data presented in Table 1. Results generated without consideration of the scattering effect are presented with the "exact" numerical results to illustrate the importance of the scattering effect.

For particles with small radius ($r = 0.1$ μm) for which the scattering albedo is small ($\omega < 0.1$), scattering has no effect on the particle emittance. ϵ_p increases with temperature because the absorption coefficient increases with increasing size parameter ($\alpha = 2\pi r/\lambda$) in the small particle size range. As the particle size increases, the scattering albedo increases ($\omega > 0.5$ for particle with radius greater than 1 μm) and the "no-scattering" results are in significant error when the particle concentration is large. Except for the lower temperature range, scattering also reduces the effect of temperature on ϵ_p because the variation of the scattering albedo with the size parameter is, in general, less than that of the absorption coefficient.

In the optically thick limit ($D \to \infty$ with optical properties kept constant), the spectral AMBL approaches a finite optically thick ($aD > 5.0$) distribution as shown in Fig. 2. Physically, scattering reduces the contribution of the particle emission to a layer of thickness AMBL. At a given wavelength λ, a scattering optically thick particle/gas layer thus behaves as a nongray emitter with

$$\epsilon_{p,\infty,\lambda} = 1 - e^{-aL_{ab}(\omega_\lambda)} \tag{14}$$

and the particle emittance is reduced to less than unity. Since the scattering albedo is based on the optical properties of the mixture, the presence of an absorbing gas has an important effect on the particle emittance. The emittance can also be a function of temperature because of the temperature dependence of the gas absorption coefficient. As an illustration, $\epsilon_{p,\infty,\lambda}$ for a particle–N_2 mixture and that for a particle–CO_2 mixture (with total gas pressure of 1 atm) at the center of the five CO_2 absorption bands are tabulated in Table 2.

3.2 Particle Attenuated Gas Emittance. The effect of temperature, particle radius, and particle number density on the particle attenuated gas emittance, $\tau_p\epsilon_g$, is illustrated by numerical data presented in Table 3. In contrast to its effect on the particle emittance, scattering increases the particle attenuated gas emittance. Mathematically, the increase in $\tau_p\epsilon_g$ is due to the reduction of AMBL caused by the scattering effect. The particle transmissivity, $e^{-a_{p,\lambda}L_{ab,\lambda}(a_{t,\lambda},\omega_{t,\lambda})}$, is increased by scattering while the gas emission effect, $1 - e^{-a_{g,\lambda}L_{ab,\lambda}(a_{t,\lambda},\omega_{t,\lambda})}$, is reduced by scattering. Since the gas emission effect is essentially optically thin except near the center of an absorption band, the increase in the particle transmissivity dominates and leads to a larger value for the particle attenuated gas emittance.

Table 3 Effect of temperature and number density on particle attenuated gas emittance, $\tau_p\epsilon_g$ (values in parentheses are generated ignoring the effect of scattering)

particle radius = 0.1 μm						
	T = 500 K	1000 K	1500 K	2000 K	2500 K	3000 K
ND = 0	0.164	0.189	0.156	0.114	0.0826	0.0605
10^{12}	0.164 (0.164)	0.189 (0.189)	0.155 (0.155)	0.114 (0.114)	0.0824 (0.0823)	0.0603 (0.0603)
10^{13}	0.162 (0.162)	0.185 (0.185)	0.151 (0.151)	0.111 (0.110)	0.0797 (0.0796)	0.0582 (0.0582)
10^{14}	0.147 (0.147)	0.155 (0.155)	0.120 (0.120)	0.0849 (0.0847	0.0598 (0.0595)	0.0429 (0.0427)
particle radius = 1 μm						
	500 K	1000 K	1500 K	2000 K	2500 K	3000 K
ND = 0	0.164	0.189	0.156	0.114	0.0826	0.0605
10^{10}	0.161 (0.161)	0.186 (0.186)	0.153 (0.152)	0.112 (0.112)	0.0809 (0.0808)	0.0592 (0.0591)
10^{11}	0.141 (0.141)	0.159 (0.158)	0.129 (0.128)	0.0940 (0.0931)	0.0674 (0.0667)	0.0490 (0.0484)
10^{12}	0.0818 (0.0717)	0.0910 (0.0718)	0.0705 (0.0518)	0.0487 (0.0336)	0.0335 (0.0219)	0.0235 (0.0147)
particle radius = 10 μ m						
	500 K	1000 K	1500 K	2000 K	2500 K	3000 K
ND = 0	0.1637	0.1893	0.1555	0.1143	0.0826	0.0605
10^{8}	0.161 (0.161)	0.186 (0.186)	0.153 (0.152)	0.112 (0.112)	0.0809 (0.0807)	0.0591 (0.0591)
10^{9}	0.140 (0.139)	0.160 (0.159)	0.129 (0.128)	0.0939 (0.0930)	0.0674 (0.0666)	0.0489 (0.0483)
10^{10}	0.0847 (0.0678)	0.0927 (0.0715)	0.0709 (0.0516)	0.0485 (0.0334)	0.0332 (0.0216)	0.0232 (0.0145)

Table 4 Effect of temperature and number density on total emittance, ϵ_t (values in parentheses are generated ignoring the effect of scattering)

particle radius = 0.1 μm						
	500 K	1000 K	1500 K	2000 K	2500 K	3000 K
ND = 0	0.164	0.189	0.156	0.114	0.0826	0.0605
10^{12}	0.166 (0.166)	0.194 (0.194)	0.166 (0.166)	0.130 (0.130)	0.104 (0.104)	0.0867 (0.0862)
10^{13}	0.182 (0.182)	0.239 (0.239)	0.253 (0.252)	0.256 (0.255)	0.262 (0.261)	0.271 (0.270)
10^{14}	0.324 (0.324)	0.489 (0.490)	0.624 (0.631)	0.703 (0.723)	0.746 (0.785)	0.767 (0.829)
particle radius = 1 μm						
	500 K	1000 K	1500 K	2000 K	2500 K	3000 K
ND = 0	0.164	0.189	0.156	0.114	0.0826	0.0605
10^{10}	0.196 (0.195)	0.221 (0.221)	0.187 (0.186)	0.146 (0.145)	0.115 (0.114)	0.0930 (0.0921)
10^{11}	0.398 (0.398)	0.422 (0.424)	0.387 (0.390)	0.351 (0.353)	0.325 (0.327)	0.308 (0.310)
10^{12}	0.788 (0.910)	0.764 (0.946)	0.734 (0.939)	0.720 (0.937)	0.713 (0.935)	0.711 (0.934)
particle radius = 10 μm						
	500 K	1000 K	1500 K	2000 K	2500 K	3000 K
ND = 0	0.164	0.189	0.156	0.114	0.0826	0.0605
10^{8}	0.194 (0.193)	0.220 (0.219)	0.189 (0.188)	0.151 (0.150)	0.122 (0.121)	0.101 (0.100)
10^{9}	0.388 (0.390)	0.418 (0.420)	0.400 (0.402)	0.381 (0.382)	0.368 (0.368)	0.359 (0.358)
10^{10}	0.743 (0.945)	0.769 (0.950)	0.771 (0.944)	0.778 (0.948)	0.784 (0.950)	0.790 (0.951)

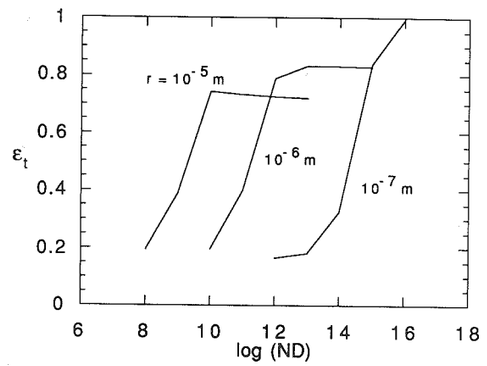

Fig. 5 Total emittance of a particle/CO_2 mixture at 500 K

Physically, this increase in the particle attenuated gas emittance can be attributed to the fact that scattering limits the mixture's contribution to the total heat transfer to within a layer of finite absorption optical thickness. Since particle absorption is the dominant effect, the particle attenuated gas emittance increases even though the region of particle emission decreases.

3.3 Total Emittance. Numerical data for the total emittance are presented in Table 4. Since the scattering effect simultaneously increases the particle attenuated gas emittance and decreases the particle emittance, its effect on the total emittance varies strongly with the particle size and temperature. For moderate and large particle sizes (1 and 10 μm), scattering reduces the optically thick limiting value of the total emittance to less than unity. Since the limiting value can be as low as 0.711 ($ND = 10^{12}$ 1/m^2, particle radius = 1.0 μm, $T = 1000$ K), this effect is quite appreciable and should not be ignored in practical engineering applications. At the low temperature limit (500 K) and high particle concentration (beyond the range shown in Table 4), the effect of scattering leads to the unusual behavior that the total emittance does not increase monotonically with increasing particle concentration. This behavior is illustrated graphically in Fig. 5.

4 Conclusion

The absorption mean beam length (AMBL) is demonstrated to be an effective concept in generating accurate prediction of the emittance of an absorbing, emitting, and scattering particle–gas mixtures. Numerical data for a carbon particle/CO_2 slab is presented to provide benchmark solution for this class of problem and to demonstrate the effect of scattering on the mixture's emittance.

The effect of scattering is shown to be very important and leads to qualitative behavior which differs significantly from the traditional no-scattering results. Specifically, the traditional concept that an optically thick particle–gas mixture is effectively black is shown to be incorrect. A mixture of large carbon particles ($r = 1$, 10 μm) has an emittance of less than unity in the optically thick limit (large particle number concentration). At low and moderate temperature, the mixture's emittance can become a nonmonotonic function of the particle concentration due to the scattering effect. The mixture's emittance first increases with particle concentration, becomes a maximum at a finite particle number concentration, and then decreases toward a lower limiting value.

Acknowledgments

This paper is based upon work supported by the National Science Foundation under Grant No. CTS-8915042.

References

Bohren, C. F., and Huffman, D. R., 1983, *Absorption and Scattering of Light by Small Particles*, Wiley, New York.

Edwards, D. K., Glassen, L. K., Hauser, W. C., and Tuchscher, J. S., 1967, "Radiative Heat Transfer in Nonisothermal Nongray Gases," ASME JOURNAL OF HEAT TRANSFER, Vol. 89, pp. 219–229.

Felske, J. D., and Tien, C. L., 1973, "Calculation of the Emissivity of Luminous Flames," *Combustion, Science and Technology*, Vol. 7, pp. 25–31.

Hottel, H. C., 1927, *Transaction American Institute of Chemical Engineers*, Vol. 19, p. 173.

Hoteel, H. C., and Sarofim, A. F., 1967, *Radiative Transfer*, McGraw Hill, New York.

Howell, J. R., and Perlmutter, M., 1964, "Monte Carlo Solution of Radiative Heat Transfer in a Nongray Nonisothermal Gas With Temperature Dependent Properties," *AIChE Journal*, Vol. 10, No. 4, pp. 562–567.

Menguc, M. P., and Viskanta, R., 1986, "An Assessment of Spectral Radiative Heat Transfer Prediction for a Pulverized Coal-Fired Furnace," *Heat Transfer—1986*, Vol. 2, pp. 815–820.

Phillips, H. R., 1977, "Infrared Optical Properties of Graphite," *Physical Review B*, Vol. 16, No. 6, p. 2896.

Skocypec, R. D., and Buckius, R. O., 1984, "Total Hemispherical Emissivity for CO_2 or H_2O Including Particulate Scattering," *International Journal of Heat and Mass Transfer*, Vol. 27, No. 1, pp. 1–13.

Van der Hulst, H. C., 1957, *Light Scattering by Small Particles*, Wiley, New York.

Viskanta, R., and Menguc, M. P., 1987, "Radiation Heat Transfer in Combustion Systems," *Progress in Energy and Combustion Science*, Vol. 13, pp. 97–160.

Yuen, W. W., 1990, "Development of a Network Analogy and Evaluation of Mean Beam Lengths for Multi-dimensional Absorbing/Isotropically-Scattering Media," ASME JOURNAL OF HEAT TRANSFER, Vol. 112, pp. 408–414.

Yuen, W. W., and Takara, E., 1990, "Development of a Generalized Zonal Method for the Analysis of Radiative Heat Transfer in Absorbing and Anisotropically-Scattering Media," *Numerical Heat Transfer*, K. Vafai and J. L. S. Chen, eds., ASME HTD-Vol. 130, pp. 123–132.

Yuen, W. W., 1991, "Scaling of Radiative Heat Transfer Effect in High Temperature Absorbing, Isotropically-Scattering Systems (Concepts of Absorption and Extinction Mean Beam Length," *Proceedings of the 4th International Symposium of Transport Phenomena in Heat and Mass Transfer*, Sydney, Australia, Vol. 3, pp. 1188–1198.

Y. R. Sivathanu

J. P. Gore

Thermal Sciences and Propulsion Center,
School of Mechanical Engineering,
Purdue University,
West Lafayette, IN 47907

Transient Structure and Radiation Properties of Strongly Radiating Buoyant Flames

Measurements of instantaneous temperature and soot volume fractions based on absorption and emission in highly buoyant turbulent acetylene/air and propylene/air flames are reported. These measurements are used to predict mean, rms, probability density functions, and power spectral densities of spectral radiation intensities along a representative horizontal chord in the flame. The results show the presence of large quantities of relatively cold soot in the vicinity of smaller amounts of hot soot particles. The resulting inhomogeneity in the temperature of soot in the flame leads to negative cross correlations between temperature and soot volume fractions. The treatment of such correlations was found necessary for predicting the observed probability density functions and the power spectral densities of spectral radiation intensities.

Introduction

Radiation properties of turbulent pool flames burning acetylene and propylene in air have been studied in the past (Sivathanu, 1990; Sivathanu et al., 1991a). These studies used measurements of soot statistics obtained from laser absorption in conjunction with a two-level model for soot temperatures to predict mean radiation intensities. The approach provided reasonable results for propylene/air flames. However, predictions of mean radiation intensity for acetylene/air flames required the use of very low temperatures (Sivathanu, 1990). The predictions for both acetylene/air and propylene/air flames were very sensitive to the choice of the upper temperature level. The discrepancies between measurements and predictions were between 15 and 100 percent.

Sivathanu et al. (1991b) measured soot volume fractions in acetylene/air jet flames using simultaneous two-line emission data (f_{ve}) and one-line absorption data (f_{va}). A two-line emission temperature (T) was also obtained during the process. The f_{ve} measurements represent Planck-function weighted averages of soot volume fractions over the probe volume. Based on the large differences between measurements of f_{ve} and f_{va}, Sivathanu et al. (1991b) concluded that the bulk of soot particles seen by the absorption probe were at relatively low temperatures. The measured emission temperatures (T) yielded reasonable predictions of spectral intensities leaving the flames when used in conjunction with local emissivities based on f_{ve}. Use of emissivities based on f_{va} led to a substantial overprediction of radiation intensities. Furthermore, the cross correlations between f_{ve} and T were found to be important in the determination of the radiation intensity.

Turbulence radiation interactions (the effect of fluctuations in scalar properties on mean radiation intensities recognized in several publications: Kabashnikov and Kmit, 1979; Grosshandler and Joulain, 1986; Gore and Faeth, 1988) were treated differently in the work reported by Sivathanu et al. (1991a, 1991b). In the earlier work (Sivathanu et al., 1991a) the turbulence properties of soot volume fractions were treated by using simultaneous two-point transient absorption measurements to account for temporal and spatial correlations. The turbulent fluctuations in temperature were not measured simultaneously. A temperature–soot volume fraction state relationship model involving two temperature levels was used. The level of temperature associated with each soot volume fraction measurement was based on an underfire-overfire intermittency inferred from a single-line emission intensity. Recently, Sivathanu et al. (1991b) have used simultaneous single point measurements of emission temperatures (T) and soot volume fractions (f_{ve}) to obtain improved predictions of radiation intensities for diametric paths in acetylene/air jet flames. The treatment of turbulence-radiation interactions included temporal autocorrelations and single point cross-correlations between f_{ve} and T.

The objective of the present work was to apply the experimental and theoretical methods developed by Sivathanu et al. (1991b) to highly buoyant turbulent acetylene/air and propylene/air flames. This application is interesting since these flames represent a longer residence time limit for radiative heat loss compared to the jet flames studied by Sivathanu et al. (1991b). It is also of interest to determine whether the findings regarding the large quantities of cold soot and the negative cross-correlations between temperatures and soot volume fractions apply to pool flames. Finally, Sivathanu et al. (1991b) reported measurements and predictions of mean and rms spectral radiation intensities, while the present paper includes Probability Density Functions (PDF) and Power Spectral Density (PSD), providing a relatively complete description of the turbulent fluctuations.

Single point transient measurements of T, f_{va}, and f_{ve} resolved to approximately 10 mm length were obtained for several radial positions at a representative axial station above the burner. These data were used in conjunction with a bivariate simulation to predict the intensity leaving a horizontal diametric path at the axial station. Comparison between measurements of radiation intensity and the results of the bivariate simulation were used to verify the length and time scale resolution necessary for effective treatment of turbulence/radiation interactions.

Experimental Methods

The experimental apparatus consisted of a 50-mm-dia gas-fired burner similar to the one studied by Sivathanu (1990). The burner consisted of a 600 mm straight steel pipe with a 100-mm-long honeycomb section and a 50 mm layer of glass

Contributed by the Heat Transfer Division for publication in the JOURNAL OF HEAT TRANSFER. Manuscript received by the Heat Transfer Division October 1991; revision received January 1992. Keywords: Combustion, Fire/Flames, Radiation Interactions.